

## SUPPORTING INFORMATION

Perineuronal nets protect long-term memory by limiting activity-dependent inhibition from parvalbumin interneurons

Wei Shi<sup>1\*#</sup>, Xiangbo Wei<sup>1#</sup>, Xiaofei Wang<sup>1</sup>, Shuwen Du<sup>1</sup>, Weixuan Liu<sup>1</sup>, Jian Song<sup>1</sup>, Yun Wang<sup>2\*</sup>

<sup>1</sup>School of Life Science, and Department of Electronic Engineering, Tsinghua University, Beijing 100084, China.

<sup>2</sup>Department of Neurology, Institutes of Brain Science, State Key Laboratory of Medical Neurobiology and MOE Frontiers Center for Brain Science, Zhongshan Hospital, Fudan University, Shanghai 200032, China.

# These authors contributed equally to this work.

\* To whom correspondence should be addressed.

E-mail: shiwei@mail.tsinghua.edu.cn

yunwang@fudan.edu.cn

Tel.: +86 10 18511691903

This PDF file includes:

Figures. S1 to S9

Materials and Methods

## SUPPLEMENTAL FIGURES

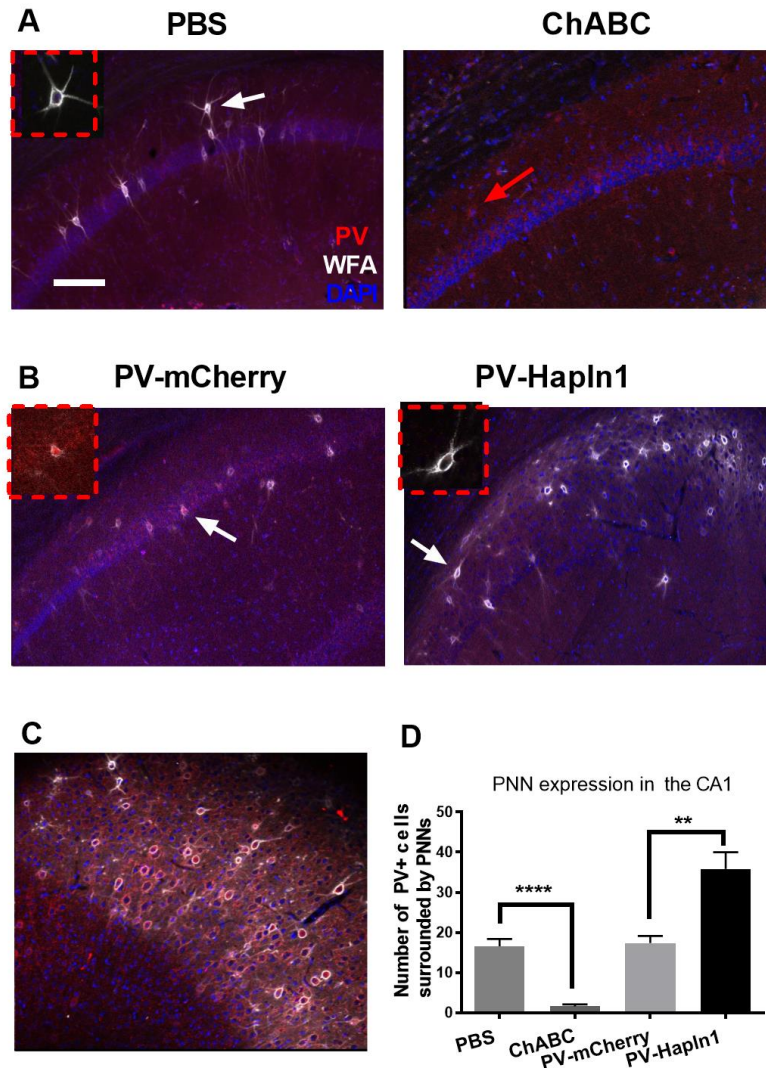


**Fig. S1 PNN expression after manipulation of PNNs.**

(A) Confocal laser scanning micrographs of WFA staining for PNN expression in PBS- and ChABC-treated mice in the hippocampus. Red arrow indicated the normal PV expression after ChABC treatment in the hippocampus. Scale bars: 100  $\mu$ m. (B) Confocal laser scanning micrographs of WFA staining for PNN expression in PV-mCherry and PV-Hapln1 treated mice in the HP. (C) Confocal laser scanning micrographs of WFA staining for normal PNN expression surrounding PV+ cells in the posterior cingulate cortex (PCC). (D) The number of PV+ cells enwrapped by PNNs in the hippocampus was significant lower in ChABC treated mice and higher in PV-Hapln1-treated mice. n=5-6 mice for each group. \*\*\*\*p < 0.0001, \*\*p < 0.01 by Student's t-test. All values are means  $\pm$  S.E.M.

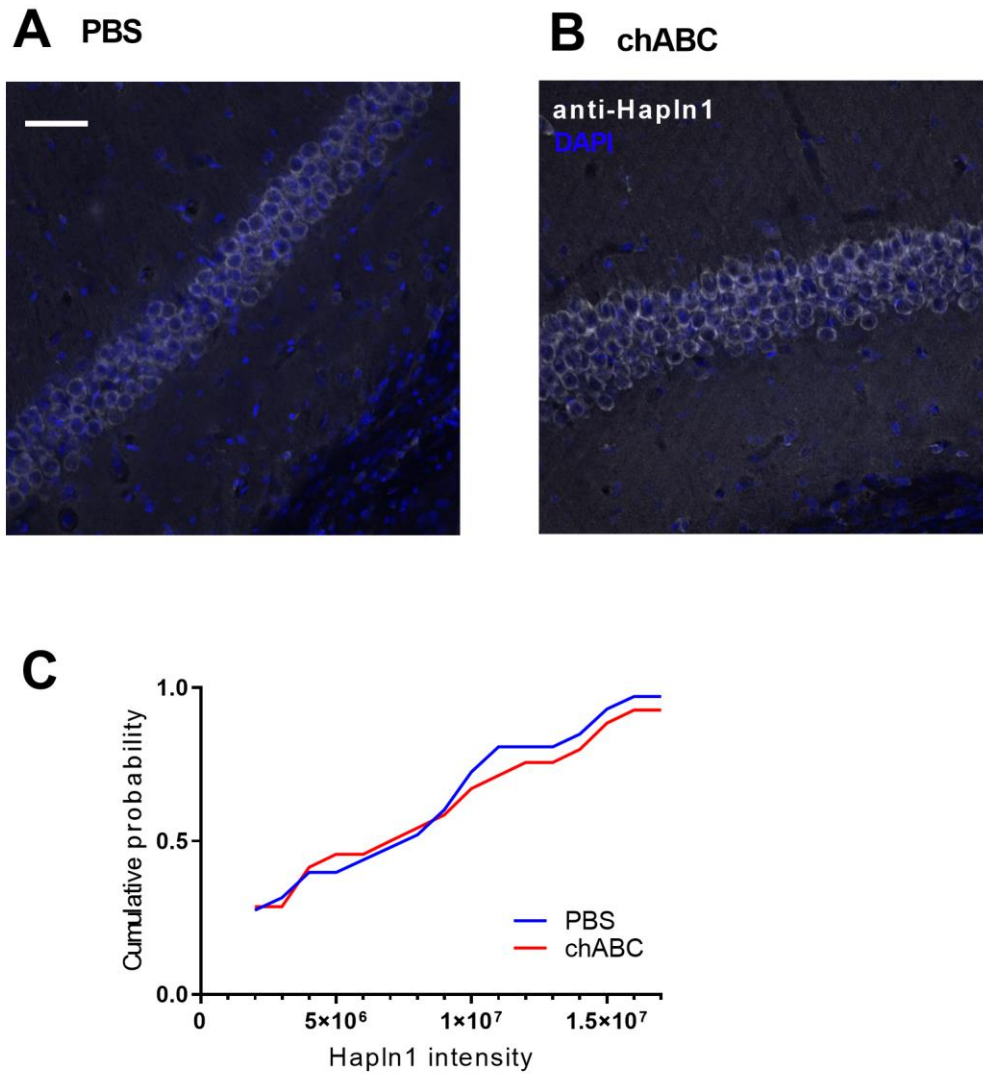


**Fig. S2 ChABC treatment did not affect Hapln1 link protein expression.**

(A, B) Confocal laser scanning micrographs of immunostaining for Hapln1 expression in PBS-treated (A) and ChABC-treated (B) mice in the HP. Scale bars: 50  $\mu\text{m}$ . (C) Cumulative probability plots of Hapln1 intensity in PBS- and ChABC-treated mice (n=24 cells, 3 mice for PBS and n=23 cells, 3 mice for ChABC).

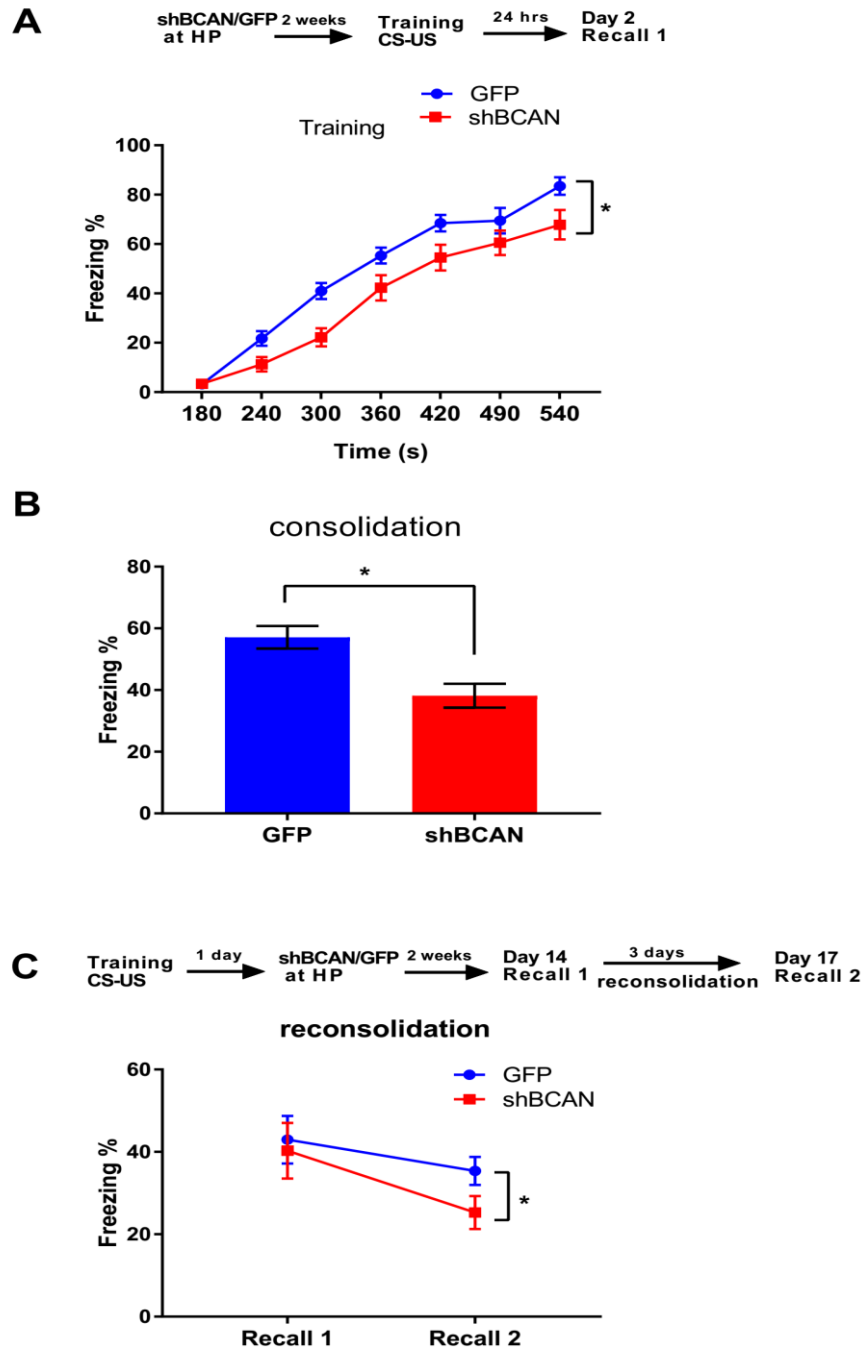


**Fig. S3. Reducing PNN expression surrounding PV interneurons in the hippocampus affected long-term contextual fear memory acquisition, consolidation and reconsolidation**

(A) Top: Schematic drawing of the experimental design for contextual fear conditioning. Bottom: Significant differences were detected in the acquisition process ( $n=15-17$  for each group). (B) Significant differences were detected in the consolidation process of recent memory after reducing PNN expression in hippocampal PV interneurons ( $n=15-17$  for each group). (C) Top: Schematic drawing of the experimental design for contextual fear conditioning. Bottom: Significant differences were detected during the recent reconsolidation process in shBCAN-treated mice in the HP after training ( $n=10$  for each group). \* $p<0.05$  by a two-way repeated measures ANOVA in (A) and (C). \* $p<0.05$  by Student's t-test in (B). All data are expressed as the mean  $\pm$ S.E.M.

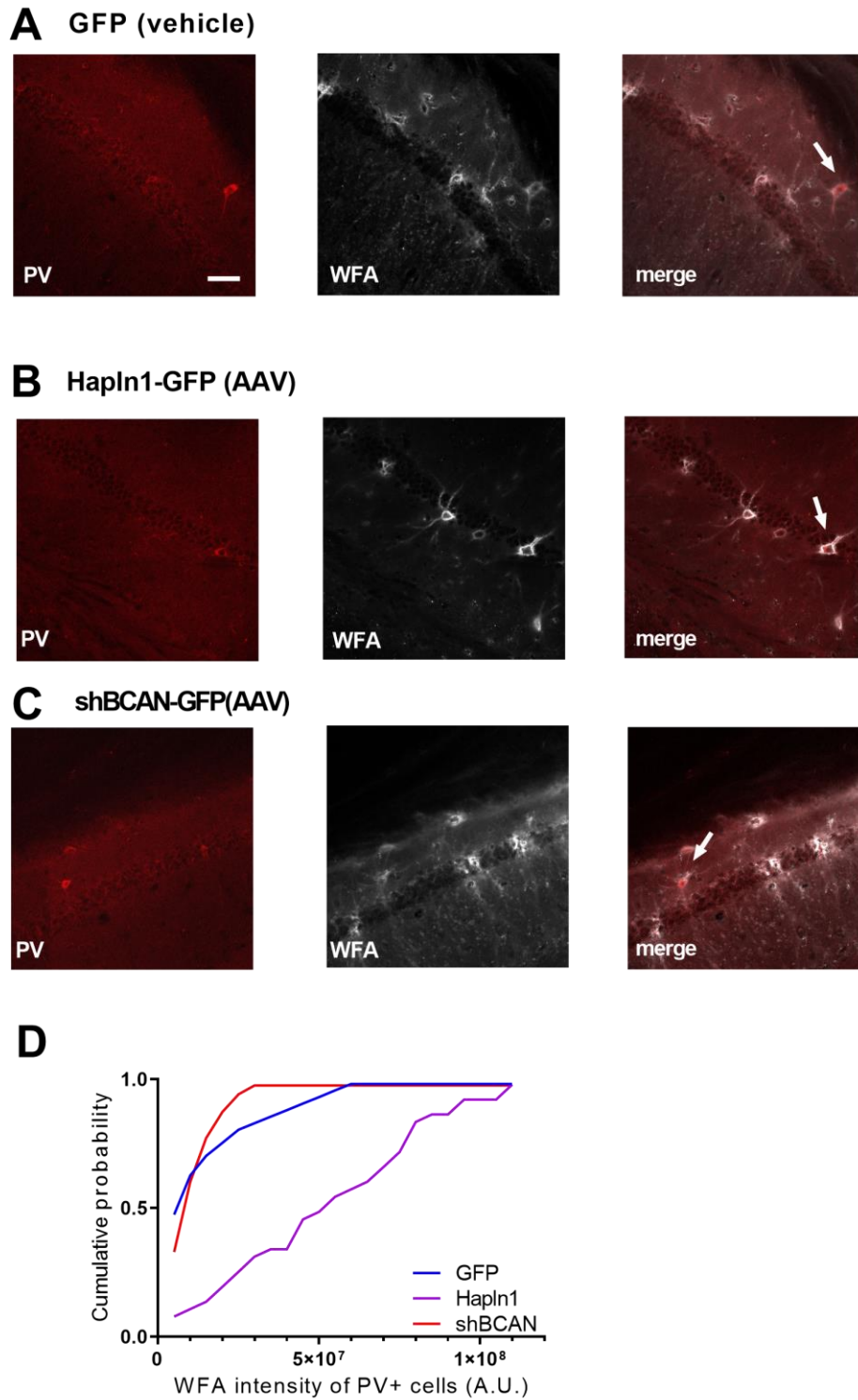
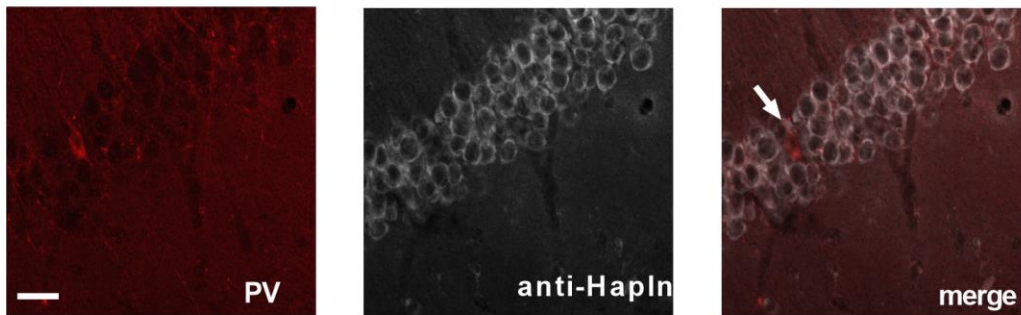


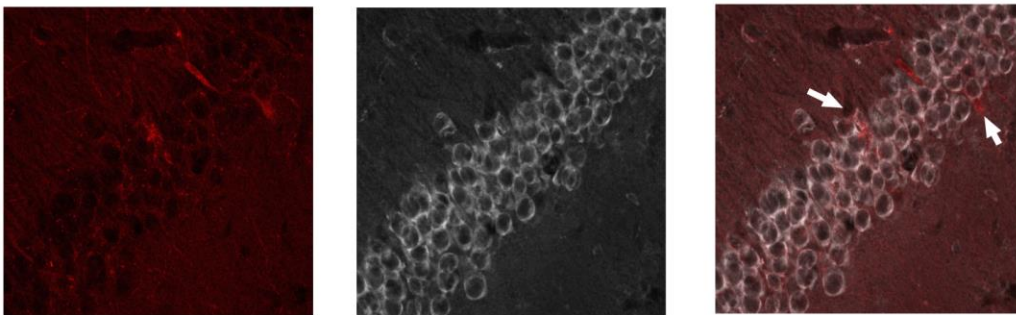
**Fig. S4 PNN expression after manipulation of PNNs of single PV cell density.**

(A) Confocal laser scanning micrographs of immunostaining for PNN expression in PV-GFP-treated mice in the HP. Scale bars: 50  $\mu$ m. (B) Confocal laser scanning micrographs of immunostaining for PNN expression in PV-Hapln1-treated mice in the HP. (C) Cumulative probability plots of WFA intensity in GFP- and PV-Hapln1-treated mice (n=34 cells, 5 mice for GFP, n=39 cells, 5 mice for Hapln1, n=29 cells, 5 mice for shBCAN).

### A GFP (vehicle)



### B Hapln1-GFP (AAV)



### C

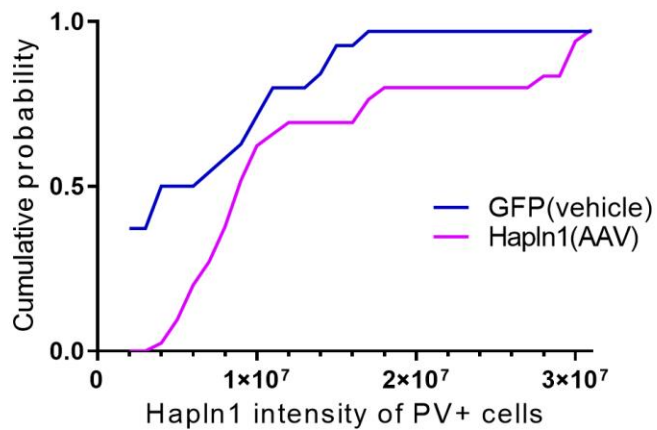


**Fig. S5 Hapln1-GFP virus treatment increased Hapln1 protein expression in single PV interneurons**

(A, B) Confocal laser scanning micrographs of immunostaining for Hapln1 expression in GFP-treated (A) and Hapln1-treated (B) mice in the HP. Scale bars: 25  $\mu\text{m}$ . (C) Cumulative probability plots of Hapln1 intensity in GFP- and Hapln1-treated mice of single PV interneurons (n=23 cells, 3 mice for GFP and n=28 cells, 3 mice for Hapln1).



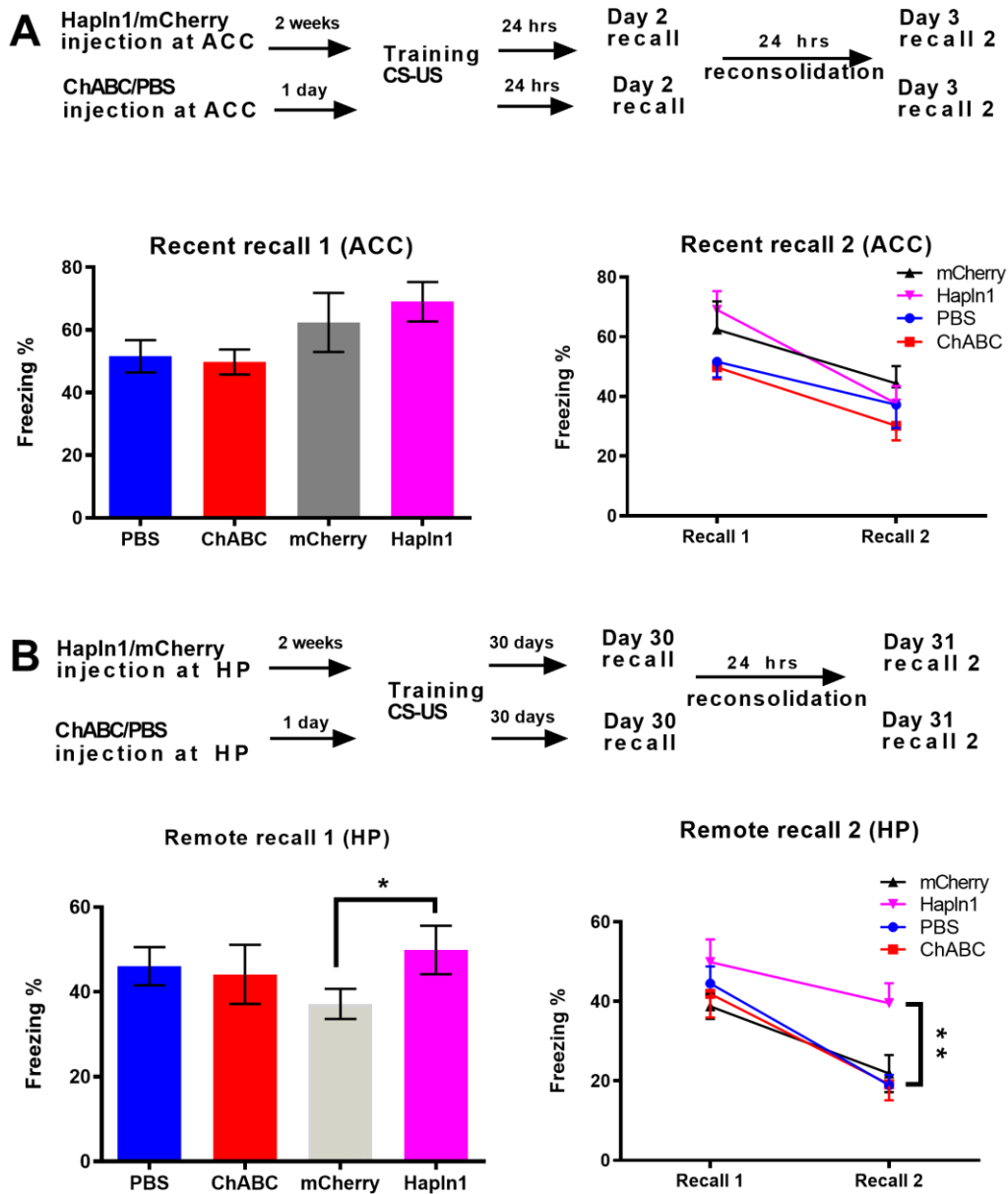


**Fig. S6. Manipulations of PNN in the ACC and the HP affected long-term recent and remote contextual fear memory consolidation and reconsolidation**

(A) Top: Schematic drawing of the experimental design for contextual fear conditioning indicating the effects of manipulation of PNNs in the ACC on the consolidation and reconsolidation process of recent memory. Left: No significant differences were detected in the consolidation and reconsolidation process ( $n=7$  for each group). (B) Top: Schematic drawing of the experimental design for contextual fear conditioning indicating the effect of manipulation of PNNs in the HP on the consolidation and reconsolidation process of remote memory. Left: Significant differences were detected in the consolidation process of remote memory after increasing PNN expression in the HP ( $n=10-12$  for each group). Right: Significant differences were detected in the ACC during the remote reconsolidation process in Hapln1-treated mice ( $n=10-12$  for each group).  $**p<0.01$  by a two-way repeated measures ANOVA. All data are expressed as the mean  $\pm$  S.E.M.

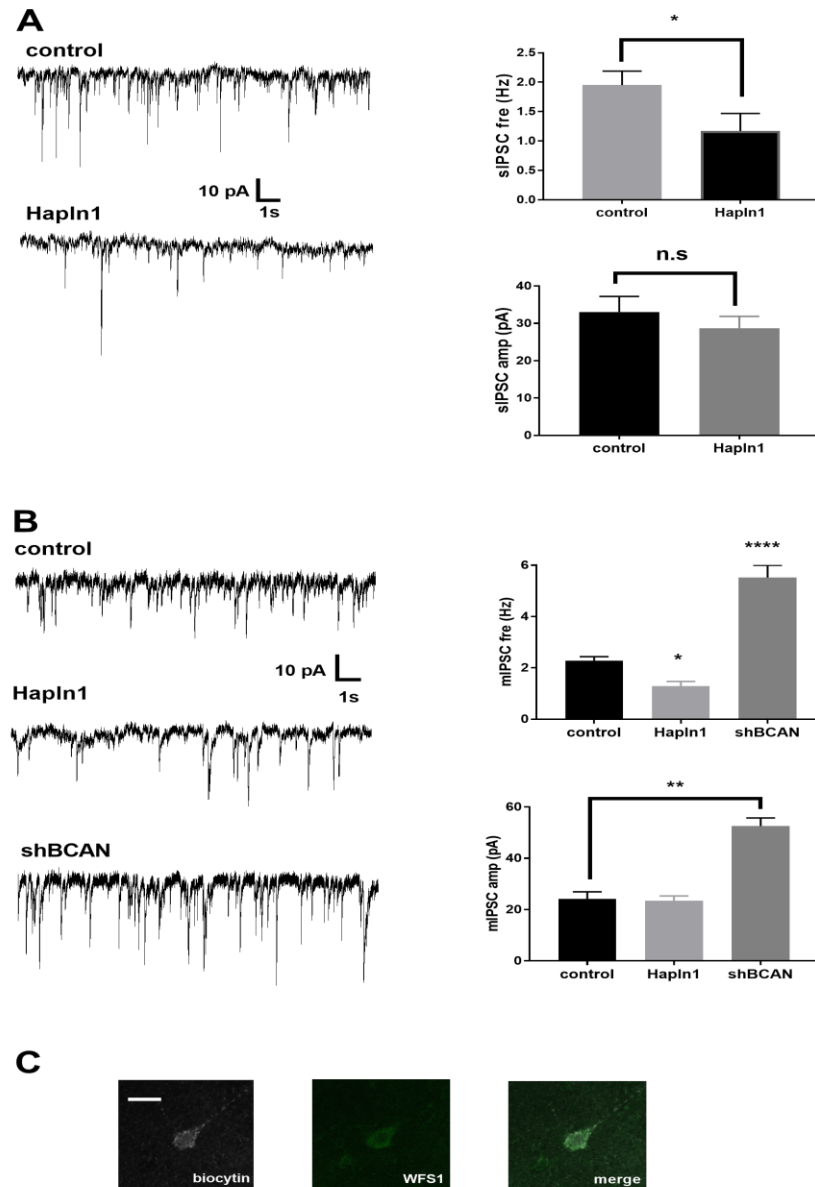


**Fig. S7 Hapln1 virus treatment decreased sIPSC and mIPSC activity in the CA1 pyramidal cells of the hippocampus**

(A) Left: Representative trace of sIPSCs from hippocampus slices of the control and Hapln1 treatment groups. Cells were voltage clamped at  $-70$  mV. Right: frequency of sIPSCs decreased significantly in Hapln1-pretreated mice compared with control mice. Bottom: Amplitude of sIPSCs showed no change in Hapln1-pretreated mice compared with control mice ( $n=8$  cells for each group). (B) Left: Representative traces of mIPSCs in control, Hapln1-treated and shBCAN-treated hippocampal slices. Cells were voltage clamped at  $-70$  mV. Right: The frequency of mIPSCs significantly decreased in Hapln1-treated mice and significantly increased in shBCAN-treated mice compared with control mice. The amplitude of mIPSCs significantly increased in shBCAN-treated mice compared with control mice ( $n=8$  cells for each group). (C) Intracellular labeling of the recorded CA1 pyramidal cells by double staining with biocytin and WFS1, a marker of pyramidal cells. Scale bar:  $20 \mu\text{m}$ . \*\*\*\* $p < 0.0001$  \*\* $p < 0.01$  \* $p < 0.05$ . All data are expressed as the means  $\pm$  S.E.M.



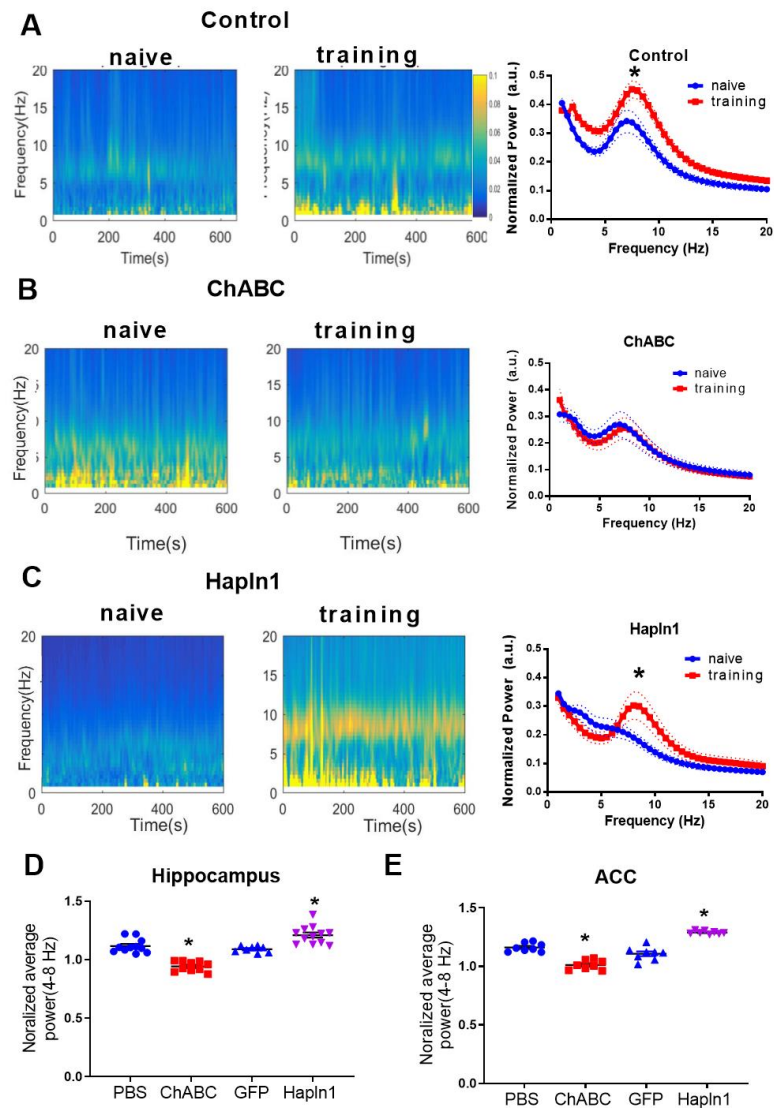


**Fig. S8. PNN affected the theta oscillations in the hippocampus and ACC after CFC training.**

(A) Left: Representative spectrograms of hippocampal LFPs during naïve and training in the control group. Right: Normalized power spectra of hippocampal LFPs recorded before and after training in the control group (n=11). (B) Left: Representative spectrograms of hippocampal LFPs during naïve and training in the ChABC-treated group. Right: Average power spectra of hippocampal LFPs recorded before and after training in the ChABC-treated group (n=10). (C) Left: Representative spectrograms of hippocampal LFPs during naïve and training in the Hapln1-treated group. Right: Normalized power spectra of hippocampal LFPs recorded before and after training in the Hapln1-treated group (n=11). (D) Normalized power spectrum of recent memory between 4 and 8 Hz after training in the PBS-, ChABC-, GFP- and Hapln1-treated mice. (E) Normalized power spectra of remote memory in ACC between 4 and 8 Hz 30 days after CFC training in PBS-, ChABC-, GFP- and Hapln1-treated mice (n=8). All data are expressed as the mean±S.E.M. Significance was tested by two-way repeated-measures ANOVA in (A), (B) and (C), \*p < 0.05, and by one-way ANOVA followed by post hoc analysis in (D) and (E), \*p < 0.05.

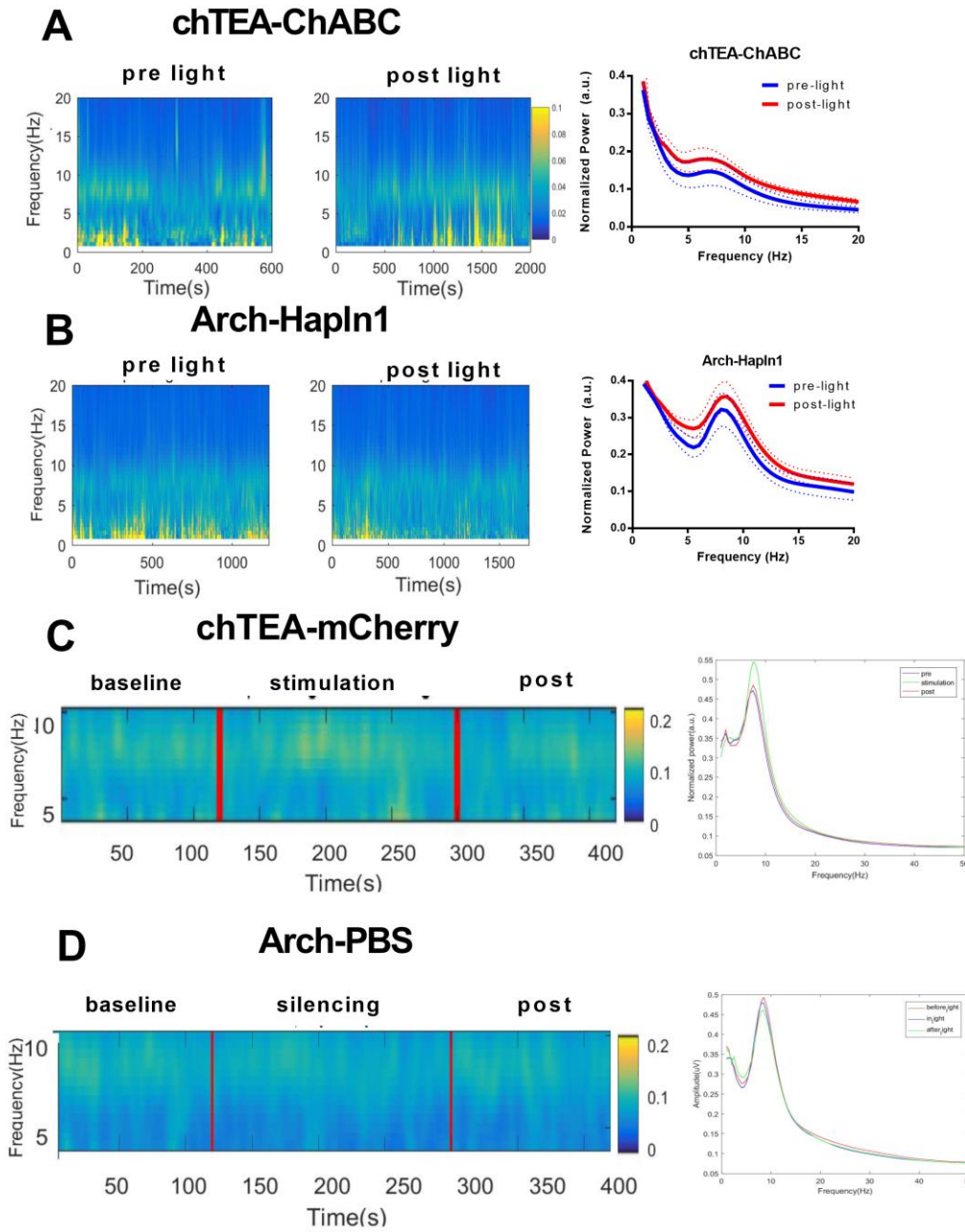


**Fig. S9 Optogenetic manipulation of PV interneurons affected theta oscillations after overexpression or removal of PNN.**

(A) Left: Representative spectrograms of hippocampal LFPs before and after light stimulation in the chTEA-ChABC group. Right: Normalized power spectrum of hippocampus LFPs recorded before and after light stimulation in the chTEA-ChABC group. (B) Left: Representative spectrograms of hippocampal LFPs before and after light inhibition in the Arch-Hapln1-treated group. Right: Normalized power spectrum of hippocampus LFPs recorded before and after light inhibition in the Arch-Hapln1 group. (C) Representative spectrograms of chTEA-expressing PV interneuron activation in the chTEA-mCherry group, showing a slight increase in the amplitude of oscillations. (D) Representative spectrograms of Arch-expressing PV interneuron inhibition in the Arch-PBS group, showing a slight increase in the amplitude of oscillations. All data are expressed as the mean $\pm$ S.E.M after two-way repeated measures ANOVA, n=5 mice in each group.

## **SUPPLEMENTAL MATERIALS AND METHODS**

### **Animal**

All experiments were performed under the Guide for the Care and Use of Laboratory Animal. The laboratory animal facility was accredited by the AAALAC (Association for Assessment and Accreditation of Laboratory Animal Care International) and the IACUC (Institutional Animal Care and Use Committee). Tsinghua University approved all animal protocols used in this study. C57BL/6J (age 3 months, male) were purchased from Vital River Laboratory (Animal Technology, Beijing, China) and were maintained under standard conditions at the Tsinghua University Animal Facility. Animals were housed in a 12 h: 12 h light-dark cycle (lights on at 7:00) with food and water provided. Animals were randomly allocated to experimental and control groups.

### **Mouse strains and genotyping**

PV-Cre knock-in mice express Cre recombinase in parvalbumin-expressing neurons without disrupting endogenous Parvalbumin expression (strain name B6.129P2-Pvalbtm1(cre)Arbr/J) come from The Jackson Laboratory (JAX 017320, USA).

### **DNA constructs and pAAV production**

All plasmids were constructed by standard molecular biology procedures and subsequently verified by double-strand DNA sequencing. Postnatal neuronal expression of Crt11 is the key event triggering the formation of PNNs (1). In this study, we used overexpression of the Crt11/Hapln1 gene (ID: 12950) in the PV interneuron, which leads to increased PNN expression in the adult hippocampus (Fig. S1; Fig. S4). pAAV-EF1a-dio-hapln1-mCherry and pAAV-EF1a-dio-hapln1-GFP were subcloned and synthesized from the Hapln1 gene (2). pAAV-EF1a-dio-EGFP, pAAV-dio-Arch3-EGFP, AAV-EF1a-DIO-chTEA -YFP-WPRE, pAAV-CaMKII-oChief and pAAV-CaMKII-eArch3 viruses were provided by BrainVTA Co., Ltd, Wuhan, China. pAAV-hysn-shBCAN-GFP virus was constructed by GeneChem Co., Ltd. (Shanghai, China).

### **Stereotactic surgery procedure**

Surgeries were performed as previously described (3). Briefly, mice were anesthetized with 0.2% sodium pentobarbital (5 ml/kg) (RWD Life Science, Shenzhen, China) and placed in a stereotaxic instrument (RWD, Shenzhen, China). The animals were given injections of sterile 0.9% NaCl throughout the surgery to reduce dehydration (1-1.5 ml/h of anesthesia). The scalp was shaved and cleaned, and a longitudinal incision was made in the skin to expose the skull. Bilateral craniotomies were preimplanted into the hippocampal CA1 or ACC region. The virus was injected using a 10- $\mu$ l nanofil syringe controlled by an Ultra Micro Pump (UMP3) with a Micro4 controller system (WPI, Sarasota, Florida, USA) at a speed of 70 nl/min. The hippocampal CA1 injections were bilaterally targeted to -2.0 mm AP,  $\pm$ 1.5 mm ML, and -1.5 mm DV(3). The coordinates used for the ACC were AP 2.0 mm, ML  $\pm$ 0.5 mm relative to the bregma and DV 1.6 mm relative to the surface of the brain (4). A volume of 300 nl pAAV-EF1a-dio-Hapln1-mCherry (pHapln1) was injected into the CA1 at a speed of 70 nl/min, and a volume of 200 nl was injected into the ACC. After injection, the needle remained in place for 5 min to ensure that the virus spread at the target location before the needle was slowly withdrawn, after which the wound was cleaned and sutured shut. The mice remained on an electric blanket until they fully recovered from the anesthesia. After surgery, the mice were allowed to recover for at least 2 weeks before all subsequent experiments were performed.

### **Chondroitinase ABC (ChABC) treatment**

Protease-free chondroitinase ABC (ChABC, C3667, Sigma) was dissolved in filtered 0.1 M PBS to a final injection concentration of 200 U/ml; aliquots were stored in -20 C and thawed immediately before use(5,6). For infusion of ChABC or vehicle (0.1 M PBS) by the preimplanted bilateral guided cannula (RWD Life Science, Shenzhen, China) in the behavior test, the dummy cannula was removed and a 33-gauge injection cannula was inserted. The injection cannula was connected to a micro syringe driven by a micro infusion pump. Animals were given bilateral intrahippocampal injections of 0.3  $\mu$ l or ACC injections of 0.2  $\mu$ l at a constant rate of

0.1  $\mu$ l/min. The injection cannula was left in place for 2 min before withdrawal.

### **Effects of optogenetic manipulation of hippocampus PV neurons and PNNs on contextual fear memory consolidation**

To specifically activate and inactivate the PV interneurons in the CA1 of hippocampus, 300 nL of AAV9-EF1a-dio-chTEA-YFP (BrainVTA, Wuhan, China) was injected into the hippocampus of the C57BL/6 PV-cre mice at the following coordinates: AP, -2.0 mm; ML,  $\pm$ 1.5 mm; and DV, -1.5 mm. For inactivation of PV interneurons, 300 nL of AAV9-Dio-eArch-EGFP (BrainVTA, Wuhan, China) virus was bilaterally injected into the hippocampus of adult C57BL/6J PV-cre mice at the same coordinates listed above. For the optogenetic protocol, the implanted optic fiber was connected to a blue or yellow light laser via patch cords (Fiblaser, Shanghai, China) and a fiber-optic rotary joint (Doric Lenses, Quebec, Canada) that allowed release of fiber torsion resulting from rotation of the mouse. For all optogenetic experiments 20 ms, 10-15 mW, 473 nm light pulses at 8 Hz for 3 min with 3 sweep 2-min intervals were delivered via a solid-state laser (Shanghai Laser & Optics Century, Shanghai, China) triggered by a stimulator (Model 2100, Isolated pulse stimulator, A-M systems, Sequim, WA, USA) or 500 ms, 10-15 mW, 586 nm light pulses at 1 Hz for 3 min with 3 sweep 2-min intervals were delivered via a solid-state laser (Inper, Hangzhou, China) for light silencing . Mice were subjected to LFP recording for 30 min after the light protocol.

### **Double immunofluorescence**

Mice were sacrificed with an overdose of pentobarbital sodium (i.p. Sagatal; RWD Life Science, Shenzhen, China) and perfused with 4% PFA. The brain was carefully removed, postfixed for 2-4 h and dehydrated overnight in sucrose (30%)-phosphate buffer (PB, 0.2 M, pH 7.4) at 4°C. The hippocampus was then cut into 80- $\mu$ m-thick coronal serial sections with a freezing microtome (VTS3000, Leica, USA). The hippocampus slices were incubated with a mixture of biotinylated Wisteria floribunda agglutinin (WFA, 1:200, L1516, Sigma or Hapln1, 1:200,

ab81997, Abcam, Cambridge, USA) and PV (1:1000, P3088, Sigma). The mixtures were then diluted with PBS with 5% BSA and incubated in PBS containing 5% BSA and 0.2% Triton X-100 for 2 h to block nonspecific binding. Slices were incubated overnight at 4° C in primary antibodies. The day after incubation, slices were incubated in a mixture of fluorochrome-conjugated immunoreagents (rhodamine-conjugated secondary IgG, 1:1000, Molecular Probes; Alexa Fluor 647, 1:1000, Abcam; DyLight® 649 Streptavidin, 1:200, SA5649, Vector, Burlingame, CA, USA) for 2 h at room temperature in the dark. Between each step, the hippocampal slices were rinsed with PBS 3 times (10 min/time). The hippocampal slices were mounted and cover slipped using mounting medium with DAPI (H1200, Vector, Burlingame, CA, USA). Then, the slices were observed under a laser scanning confocal microscope (LSM710META, Zeiss, German), and a CCD camera connected to a computer was used to capture digital images for further analysis.

### **Image acquisition and analysis**

The purpose of our study was to determine the trends in relative changes in PNN expression (detected by WFA staining) before and after training. WFA/PV positive cell counts in the hippocampus CA1 were delineated by image detection software (Imaris 9.2, Bitplane AG). Samples belonging to the same experiment were imaged during the same imaging session on an inverted Zeiss LSM 710 confocal microscope. Imaging was performed with the same laser power, photomultiplier gain, pinhole, and detection filter settings (1024x1024 resolution, 12 bits or 16 bits). For WFA and PV level analyses, AF647 and Cy3 and fluorophores were used, respectively, and confocal image stacks (40X immersion objective, 1.4 NA, 0.2 µm step size) were reconstructed and analyzed with IMARIS 9.2 software. WFA-positive neurons within the tissue sections with optimal staining were isolated in three dimensions. Three-dimensional isosurfaces were created around each neuron using the “create surface” tool, and volume and labeling intensities were quantified automatically. A threshold was selected to include as much of the neuron as possible while excluding any background. A size filter was applied with the minimum size



being related to the volume of the cell. The WFA surface was then used to define the cellular domain and create three-dimensional isosurfaces around the neuron in the WFA channel. WFA volume and intensity were quantified automatically. For the PV soma, a color threshold was selected to identify the cell soma. The border of the soma was automatically or manually drawn to calculate its perimeter and create a mask of only the cell body. The PV cell soma was detected with the “spot” tool using a spot diameter of 0.68 mm. A threshold was selected to accurately detect as many spots as possible without creating artifacts. The radius of the spot was used as a threshold distance to define the contact, and the “Find spots close to surface” tool (ImarisXT extension) was then used to count the number of WFA surface and PV spots that were contacting the surface of the soma.

### ***In vitro* slice preparation and electrophysiology**

To study the slow developing (delayed) effects of ChABC, ChABC was injected (200 U/ml) onto the CA1 area in vivo 24 h before the animals were decapitated. Acute 300  $\mu$ m transverse hippocampal slices were prepared using a vibratome (VF300, Precisionary Instruments, USA). The slices were maintained at room temperature in a submersion chamber with artificial cerebrospinal fluid (ACSF) containing (in mM) 125 NaCl, 2.5 KCl, 2 CaCl<sub>2</sub>, 1 MgCl<sub>2</sub>, 1.25 NaH<sub>2</sub> PO<sub>4</sub>, 24 NaHCO<sub>3</sub> (PH=7.4), and 15 glucose, bubbled with 95% O<sub>2</sub>/5% CO<sub>2</sub>. Slices were incubated for at least 1 h before removal for experiments. Slices were kept in MED probe for 1 h for attachment with the 16-channel array (MED-PG515A, Alpha MED Sciences) (preheated to 33°C), where they were superfused with oxygenated ACSF. Extracellular field excitatory postsynaptic potentials (fEPSPs) in the Schaffer collateral pathway were synaptically evoked at 0.025 Hz and recorded in the CA1. fEPSPs were evoked using a stimulation intensity that elicited a 30% maximal response. Data acquisition and analysis were performed using the multielectrode MED64 hardware and software packages (Panasonic, Japan). Additional analyses were performed using custom macros running under Igor Pro. LTP was induced by 1-train theta burst stimulation (TBS) consisting of 1 epoch of 10 trains of 5 bursts repeated at 5 Hz, delivered at the same intensity of baseline recording. Researchers

did not perform data collection and analysis blinded to the conditions of the experiments.

### **Whole-cell patch-clamp experiments**

To provide examples of the morphology of recorded neurons, glass pipettes were filled with intracellular recording solution containing 0.5% biocytin (Sigma-Aldrich, Darmstadt, Germany). The recording slices were incubated with parvalbumin primary antibody or Wolfram syndrome protein (WFS1) antibody (26995-1-AP, Proteintech, Rosemont, USA) and secondary antibody after overnight fixation with PFA. The recorded neurons devoid of parvalbumin-immunoreactivity or WFS1-positive neurons are pyramidal neurons (7). Patch pipettes (4-6 M $\Omega$ ) were pulled from borosilicate glass capillaries on a P1000 puller (P1000, Sutter Instrument) and were filled with an internal solution containing (in mM): 140 KCl, 2 MgCl<sub>2</sub>, 2 Na<sub>2</sub>ATP, 1 ethylene glycol-bis (b-aminoethyl ether)-N,N,N',N-tetra-acetic acid (EGTA) and 10 N-2-hydroxyethylpiperazine-N'-2-ethanesulphonic acid (HEPES), pH 7.3, 285-295 mOsm. The CsCl-based internal solution was used to record most evoked inhibitory postsynaptic currents (eIPSCs). The pipette was advanced towards the soma of the target cell by the micromanipulator (MP-285, Sutter Instruments, Novato, USA). The recorded signals were digitized at 10 kHz and filtered at 3 kHz by a Multiclamp 700A amplifier, Digidata 1322A analog/digital interface board and pCLAMP 10.2 software (Axon Instruments, Molecular Devices, LLC, San Jose, USA). Normally, no series resistance compensation was applied, but the cell was rejected if the access resistance changed significantly (>25%) during the course of recording. Stimuli consisting of 100–200  $\mu$ A pulses of 0.1 ms duration were delivered at 0.05 Hz. All eIPSCs were recorded at -70 mV in regular Mg<sup>2+</sup> aCSF containing DNQX (Tocris; 10  $\mu$ M) and D-APV (Tocris; 50  $\mu$ M) to block glutamate transmission. At the same time, the glycine receptor antagonist strychnine (Sigma, 1  $\mu$ M) was also applied to record the GABA<sub>A</sub> receptor-mediated current.

After recording, the features of sIPSCs or mIPSCs were analyzed using Mini Analysis program v.6 software (Synaptosoft Inc, Fort Lee, USA). Series resistance < 20 M $\Omega$  and input resistance > 100 M $\Omega$  during recordings were included for further

analysis. The threshold for detection was set at 2-fold higher than the baseline noise. For every experiment, correct events were confirmed using visual detection. The frequency of sIPSCs or mIPSCs was measured from a continuous recording of 10 min and was calculated by dividing the total number of positive events with the recording duration. The amplitude of sIPSCs or mIPSCs was the distance from peak to baseline. The 10% rise time, 80% decay time and decay time constant were measured on a couple of single events in which no other rising and decay phases were present. After recording, eIPSCs were analyzed off-line using the Digidata-pClamp package (Axon Instruments). All amplitudes of eIPSCs recorded per minute were averaged and normalized to the baseline level (the average of all tracings before TBS) for evaluating the effect of stimulation in regular conditions or under pharmacological manipulations. The average traces of baseline eIPSCs were 10 min. The average traces of eIPSCs after application of TBS to the cell were between 10 min and 40 min. Student's paired t-test was used to compare the average amplitude of eIPSCs before and after TBS. Numerical data are presented as the mean  $\pm$  SEM (standard error mean). For every condition, paired Student's t-test was used to compare the average eIPSC amplitude before and after TBS. Data were considered statistically significant only with  $p < 0.05$ .

### **Drug application**

CNQX (6-cyano-7-nitroquinoxaline-2,3-dione) and DAP-5 (2-amino-5-phosphonopentanoic acid) were obtained from Tocris Bioscience (USA); strychnine was obtained from Sigma-Aldrich (USA). Drugs were dissolved in dimethyl sulfoxide (DMSO). To minimize the effect of DMSO in brainstem slices, the amount of DMSO in the final concentration of drugs applied was less than 0.1%. All drugs were freshly added to the ACSF or incubation medium on the day of the experiment. Drug-loaded ACSF was perfused in the recording chamber and reached the slice through a gravity-feed system.

### **Contextual fear conditioning test**

Animals were first habituated to the neutral chamber between 10:30 and 11:00 AM on two consecutive days. Thereafter, spontaneous freezing behavior was recorded as baseline by a computer using Freeze Frame software (Coulbourn Inc., USA) and a CCTV camera (Sentech USB 2 camera) for 20 min in the neutral chamber on two successive days (Kumar & Jha, 2012). The conditioning and extinction boxes and the floor were cleaned with 70% ethanol before and after each session. To score freezing behavior, an automatic infrared beam detection system placed on the bottom of the experimental chambers was used. Freezing behavior was considered if no movement was detected for 2 s, and the measure was expressed as a percentage of time spent freezing.

Twenty-four hours after ChABC or PBS injection, adult mice were submitted to discriminative fear conditioning (day 1) by pairing the CS+ (conditioning boxes) with 5 pairings of US (a 2-s foot-shock at 0.8 mA, intertrial interval: 60 s). On day 2, each animal was tested for long-term contextual fear memory by placing it back in the original training chamber and monitoring freezing behavior every 2 s for a total of 3 min. For evaluation of long-term remote memory, adult mice were conditioned by using 5 presentations of the US (a 2-s foot-shock 0.8 mA, intertrial interval: 60 s) in the conditioning boxes. Then, ChABC or PBS were injected into these conditioned mice one week or three weeks after training and submitted to a 30-day test.

### **Statistical analysis**

Two-way or one-way ANOVA followed by multiple comparison tests was used to compare the features of the electrophysiology recordings and the freezing behavior tests. All data were analyzed by Student's t-test or a post hoc test following ANOVA. Statistical results are presented as the means  $\pm$  SEM. Asterisks indicate significant values (\*P < 0.05; \*\*P < 0.01, and \*\*\*P < 0.001). n.s. indicates no significant difference (P > 0.05).

### ***In vivo* multichannel recording**

Broadband (0.3 Hz - 7.5 kHz) neural signals were simultaneously recorded (16 bits @ 30 kHz) from implanted single electrode and optofibers using a multichannel data acquisition system (Apollo, Bio-Signal Technologies: McKinney, TX, U.S.A.; Cereplex direct, Blackrock microsystem, U.S.A). Field potential bands were extracted with low-pass (200 Hz) filters. Field potentials were down sampled to 1 kHz and were used for analyzing data in Neuroexplorer (Nex Technologies: Boston, MA, U.S.A.) and in a custom-written MATLAB program (Stanford Wavelab, U.S.A). Spectra of 0-20 Hz PSD activity were normalized to the mean power of the 1-3 Hz band of each mouse. Spectrograms of 0-20 Hz PSD activity were generated in MATLAB (10 min of baseline LFP recording before light and 30 min of postlight recording). PSD data for representative LFPs were calculated in 1-s windows, and PSDs were convolved over 30 s at 1 Hz. PSDs were normalized over the entirety of the selected temporal window and expressed as  $\mu\text{V}^2\text{Hz}^{-1}$ .

## References

1. D. Carulli, *et al.*, Animals lacking link protein have attenuated perineuronal nets and persistent plasticity. *Brain* 133(Pt 8):2331-2347 (2010).
2. M. Czipri, *et al.*, Genetic rescue of chondrodysplasia and the perinatal lethal effect of cartilage link protein deficiency. *J Biol Chem* 278(40):39214-39223 (2003).
3. Y. Liu, *et al.*, Hippocampal Activation of Rac1 Regulates the Forgetting of Object Recognition Memory. *Curr Biol* 26(17):2351-2357 (2016).
4. G. Paxinos, C. Watson. *The rat brain in stereotaxic coordinates*, (Academic Press/Elsevier, Amsterdam ; Boston ;, 2007).
5. G. Bruckner, *et al.*, Acute and long-lasting changes in extracellular-matrix chondroitin-sulphate proteoglycans induced by injection of chondroitinase ABC in the adult rat brain. *Exp Brain Res* 121:10 (1998).
6. N. Gogolla, P. Caroni, A. Luthi, C. Herry, Perineuronal nets protect fear memories from erasure. *Science* 325(5945):1258-1261 (2009).
7. F.L. Hitti, S.A. Siegelbaum, The hippocampal CA2 region is essential for social memory. *Nature* 508(7494):88-92 (2014).